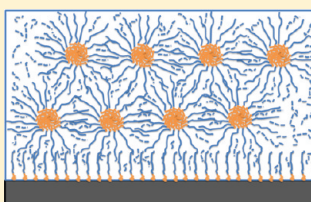


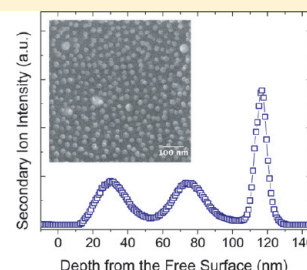
Tethered-Polymer Structures in Thin Film Polymer Melts

X. Chelsea Chen,[†] Hengxi Yang,[‡] and Peter F. Green^{*,†,§}[†]Macromolecular Science and Engineering, [‡]Departments of Physics and [§]Materials Science and Engineering, University of Michigan, Ann Arbor, Michigan 48109, United States

ABSTRACT: We show that polystyrene-*b*-poly(2-vinylpyridine) (PS-*b*-P2VP) diblock copolymer chains aggregate to form micelles, composed of an inner P2VP core and an outer PS corona, as well as adsorb onto the substrate, forming brush layers, in supported thin film PS/PS-*b*-P2VP mixtures. The degrees of polymerization of the chains that comprised the corona and core were N_{PS} and N_{P2VP} , respectively. The diameter of the micelle cores, D_{core} , increased with increasing degree of polymerization, P , of the PS host and became constant for large values of P . A decrease in the number density of micelles, $n_{micelle}$, accompanied the increase in D_{core} ; $n_{micelle}$ reached a plateau in the same range of values of P where D_{core} became constant. The organization of the micelles suggests the existence of attractive micelle–micelle interactions in the large P regime. Moreover, in this regime, the micelles preferentially migrated to the free surface. The morphology of this system is compared to thin film PS melts containing brush-coated nanoparticles. One fundamental difference between the two systems is that the micellar system has the ability to adjust the number of chains per micelle, and hence the number of micelles, in order to mediate the free chain/brush (micelle corona) interactions. This has important consequences on the location of the wet-brush to dry-brush transition.



20% polystyrene-*b*-poly(2-vinylpyridine) in thin film polystyrene



INTRODUCTION

A-*b*-B diblock copolymers, apart from self-organizing into A-rich and B-rich domains of different symmetries (cylinders, spheres, lamellae) possessing long-range order.¹ They are known to exhibit significant interfacial activity, which has the effect of modifying the behavior of different systems for various applications:^{2–12} the wettability of surfaces, stabilization of colloidal particles, enhancement of adhesion, and reducing the interfacial tension leading to an enhancement of the compatibility of dissimilar phases. When dissolved in a selective solvent, A-*b*-B copolymers will self-assemble into micelles; the micelles may be employed for applications that include the sequestration of nanoparticles¹³ as well as for drug delivery applications.^{14,15}

Micelle formation in block copolymer/homopolymer mixtures has been of interest, both theoretically^{16–21} and experimentally^{4,5,22–27} for nearly 3 decades, yet there remain important unresolved questions, particularly in relation to the role of confinement on the formation and organization of micelles. In a selective solvent environment, such as a homopolymer of type-A, the A-*b*-B diblock copolymer chains of sufficiently low concentration form micelles with an inner core composed of the B-component and a corona composed of the A-component. On the basis of the disparities between the degrees of polymerization of the two blocks, N_A and N_B , the Flory–Huggins interaction parameter χ and the concentration, micelles of different geometries may form.^{15,21,28} For example, when N_A is much larger than N_B , micelles are spherical. Leibler et al.¹⁶ calculated the free energy of formation of micelles in a copolymer/homopolymer melt under conditions where the homopolymer chains of type A, of degree of polymerization P , were sufficiently short such that they readily intermixed with the corona. They predicted that the copolymers would aggregate to

form micelles at concentrations greater than a critical micelle concentration (cmc), which is a function of χN_B , in order to minimize the unfavorable A/B contacts. The calculations were restricted to the case of symmetric copolymers, where $N_A = N_B$. Whitmore and Noolandi¹⁷ subsequently extended the work to include the effects of varying N_A , N_B , and P on the structure of the system. Shull et al.²³ showed that the micelles exhibited a tendency to migrate to interfaces in thin films, thereby demonstrating the role of micelle–interfacial interactions on the structure of the mixtures. Esselink et al.²⁴ described the interactions between deuterated polystyrene-*b*-poly(2-vinylpyridine) (dPS-*b*-P2VP) micelles in thin film polystyrene (PS) hosts, revealing the possibility of the formation of an ordered phase of micelles. More recently, Cavallo et al.²¹ used coarse-grained, Monte Carlo, lattice simulations to understand the role of an interacting interface on the structure of the copolymer/homopolymer system. They predicted a “diagram of states”, which described the conditions under which different phases (bulk and surface micelles, brush layers, free copolymer chains) would coexist.

Some time ago it was shown that symmetric polystyrene-*b*-poly(methyl methacrylate) (PS-*b*-PMMA) diblock copolymers, $P \gg N$ at concentrations below ϕ_{cmc} , segregated to the SiO_x substrate, leaving free copolymer chains in the interior of a thin film PS-*b*-PMMA:PS/ SiO_x mixture.³ In a more recent study,²⁹ our group found that PS-*b*-PMMA diblock copolymers preferentially adsorbed onto the substrate to form a brush layer at concentrations even for $\phi > \phi_{cmc}$ prior to micelle formation, provided the film was sufficiently thin. In the study described herein, we examine the

Received: January 5, 2011

Revised: May 15, 2011

Published: June 24, 2011



conditions that determine the equilibrium density and dimensions of the micelles and the brush layer thickness in thin film polystyrene-*b*-poly(2-vinylpyridine) (PS-*b*-P2VP)/PS mixtures. The effects of host molecular weight on the micellar core sizes, micelle–micelle interactions and on the corona/homopolymer interactions are discussed. The effects of the host molecular weight on the equilibrium of the system, between the copolymer chains in the micelles, those adsorbed onto the surface to form the brush layer and the free copolymer chains in the system are also examined. Finally, the behavior of these thin film systems is compared to PS thin film systems containing nanoparticles onto which PS chains of degree of polymerization N are grafted.

EXPERIMENTAL SECTION

Solutions of the diblock copolymer polystyrene-*b*-poly(2-vinylpyridine) (PS-*b*-P2VP, Polymer Source Inc.) and a series of PS homopolymer with different molecular weights, ranging between 13 000 and 1 600 000 g/mol (Pressure Chemical Co.), were prepared in toluene. The number-average molecular weights of the components of the copolymer were $M_n(\text{PS}) = 50\,900$ and $M_n(\text{P2VP}) = 29\,100$; their degrees of polymerization were $N_{\text{PS}} = 489$; $N_{\text{P2VP}} = 277$; $N = 766$ and the polydispersity index $\text{PDI} = 1.06$. These solutions were prepared such that the weight ratio of diblock copolymer to PS homopolymer was 1:4. Some solutions were spincoated onto Si_3N_4 substrates (WaferNet, Inc.), whereas others were spincoated onto glass slides, and subsequently floated onto deionized water and picked up on Si_3N_4 (grids) substrates (Structure Probe, Inc.). The thickness of the films was controlled to be 110 ± 4 nm, measured using a variable angle spectroscopic ellipsometer (J.A. Woollam Co., Inc.), and fitting the ellipsometric angles, Δ and Ψ , to a Cauchy model in the WVASE32 software. The films were subsequently dried in vacuum at 65°C for 24 h and then annealed at 160°C for 8 to 72 h.

Scanning transmission electron microscopy (STEM), using a spherical aberration corrected JEOL 2100F instrument with a high angle annular dark field detector, was used to investigate micelle formation in the films that were transferred to the Si_3N_4 grids. Prior to analysis the films were stained in iodine vapor for 10 s to 5 min in order to make the P2VP component visible. The size of the micellar cores and the number density of the micelles were calculated in ImageJ software; groups of at least 100 micelles from three different areas of each film were analyzed. The following experimental detail is worth mentioning: the size of the micelles stained in iodine vapor for 10s, 1 min and 5 min changed by less than 3%, which is within the range of experimental error; the samples examined in our experiments were stained for less than 5 min.

The depth profiles of the brush layers and the micelles (specifically the P2VP block) in the films on the Si_3N_4 wafers were measured using secondary ion mass spectroscopy (SIMS). These measurements were performed on a Physical Electronics 6650 Quadrupole instrument, by Dr. Tom Mates at the University of California, Santa Barbara. The samples that were analyzed by SIMS were of the following configuration: a thin layer of deuterated-PS is in contact with the outer surface of the copolymer homopolymer thin film mixture, which was supported by the substrate. The deuterated-PS layer is necessary to ensure a constant etch rate, hence consistency, in the SIMS experiments. Profiles of individual elements or fragments of molecules, including Si, H, D, C and CN, in the samples were readily determined by the measurement.

The brush layer was also determined using another procedure. Some films, after annealing, were exposed to a toluene (a selective solvent for PS) bath in order to expose the underlying brush layer in contact with the substrate. The films were then dried in vacuum at 65°C for overnight and then annealed at 160°C for 24 h. The thicknesses of the brush layers were then determined using ellipsometry, and independently by scanning probe microscopy (SPM, Asylum Research) after scratching them with a razor blade.

RESULTS AND DISCUSSION

In thin film A-*b*-B diblock copolymer/A-homopolymer mixtures supported by a substrate, the copolymer chains generally exhibit a tendency to aggregate to form micelles, possessing an inner core of the B-component, and an outer corona of the A-component. Additionally, the copolymer chains may segregate to one, or both interfaces, forming a brush layer, in order to minimize the free energy of the entire system. Brush layers would be absent if the A-homopolymer chains were preferentially attracted to the substrate and to the free surface. Since PS possesses a lower surface energy than P2VP, PS resides at the free surface; the P2VP component exhibits a preferential affinity for the more polar substrate.^{23,29} In our system, micelles possessing a P2VP-core and PS-corona would form and a PS-*b*-P2VP brush layer would develop at the substrate. The STEM images in Figure 1 reveal that spherical micelles develop in all the PS hosts, regardless of their degrees of polymerization, P , after annealing. In these images, the P2VP cores appear to be bright, due to staining by iodine. Three things are evident from Figure 1 and Figure 2: (1) the micellar cores increase in size with increasing PS host molecular weight, reaching a plateau for $P \geq 5660$ ($M_n \geq 590\,000$); (2) the number density of micelles decrease with increasing P , reaching a plateau in the same regime of P where core size becomes constant; (3) the organization of the micelles exhibit hexagonally close-packed symmetry in higher molecular weight PS hosts ($P \geq 5660$, Figure 1d–f). The data in Figure 2a reveal that the average diameter of the micellar core, D_{core} , increases from 22 nm in $P = 125$ host to a value of 42 ± 5 nm for $P \geq 5660$ ($M_n \geq 590\,000$). We note that micelles were fully developed within a few hours of annealing and the size of the micelles remained constant with further annealing.

The rationale behind the decrease in diameter of the micellar cores with decreasing P is now discussed. It is known that the size of the micelles is determined by a balance between the following factors: the interfacial tension between the A and B species, which favors the formation of large micelles, the elastic energy of the copolymer chains that compose the micelles, which favors smaller micelles, and the translational entropies of the free copolymer and the homopolymer host chains.¹⁶ In the limit where $P \gg N_{\text{PS}}$, the homopolymer chains would be largely excluded from the micellar coronas. This would be the so-called “dry brush” regime. Note that a brush layer of chains grafted to a surface, under dry-brush conditions, there is a finite penetration depth, λ , between the homopolymer chains and chains end-grafted onto a surface, which is proportional to the relative length of the grafted chains to the homopolymer chains, $\lambda \sim N/P$.³⁰ In this regime the core size and the micellar size would be largest.

Shull et al.²³ showed that under conditions where $P \gg N_{\text{PS}}$ the radius of micelle core would be

$$R_{\text{core}}^3 = \frac{3}{4\pi} \frac{gQ}{\rho_0} N_{\text{core}} \quad (1)$$

and the radius of the micelle would be specified by $R_{\text{micelle}}^3 = 3QN_{\text{core}}/4\pi\rho_0$. In these equations N_{core} is the degree of polymerization of the blocks that comprise the micelle core, ρ_0 is the reciprocal of the segmental volume, $g = N_{\text{core}}/N$, where N is the total degree of polymerization of the copolymer, and Q is the number of chains per micelle, specified by

$$Q = \frac{\chi^{1/2} g \rho_0 a^3 N_{\text{core}}}{0.337 - 0.194g^{1/3}} \quad (2)$$

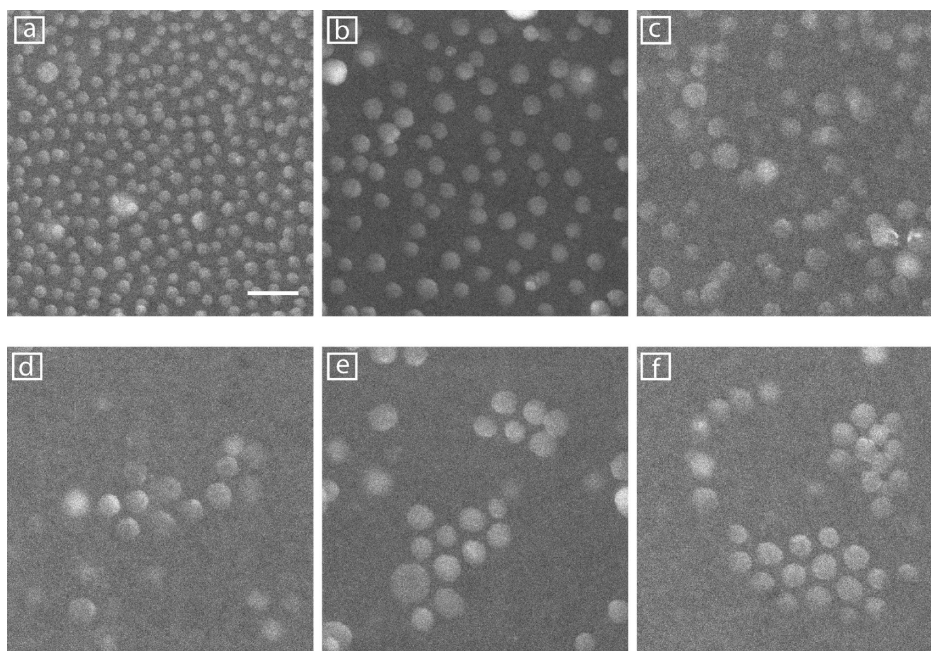


Figure 1. Scanning transmission electron micrographs (STEM) of 20% PS-*b*-P2VP in PS homopolymers with degrees of polymerization of $P = 125$ (a), 470 (b), 1460 (c), 5660 (d), 8640 (e), and 15400 (f) are shown. All films were approximately 110 nm, annealed in vacuum at 160 °C and stained in iodine vapor. Scale bar represents 100 nm.

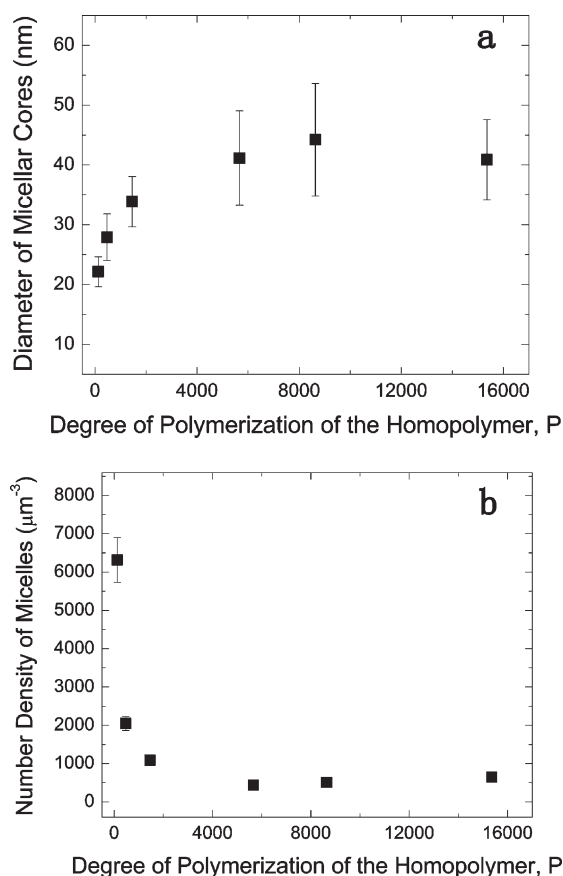


Figure 2. (a) Dependence of the micelle core diameter and (b) number density of micelles are shown here as a function of the host molecular weight.

Using the following information, $\rho_0 = 9.4 \times 10^{-3} \text{ mol/cm}^3$, $\chi = 0.11$, $a = 0.69 \text{ nm}$, $N_{\text{core}} = 277$, $N = 766$, and $g = 0.362$, we

calculated that $R_{\text{micelle}} = 30 \text{ nm}$. The micellar core diameter was calculated to be $D_{\text{core}} = 2R_{\text{core}} = 44 \text{ nm}$, which is in excellent agreement with the experimentally determined values (Figure 2a). In this regime, $P > 3N_{\text{PS}}$, the average diameter of the cores should be largest. For smaller values of P , the micellar size decreases and the number of micelles increases. We will later address these observations when we compare the behavior of this system to that of chain end-tethered surfaces, with fixed number of chains per unit area Σ_0 .

SIMS was used to determine the depth profiles of the micelles and the brush layers of copolymer chains that adsorbed to the substrates of the samples. The SIMS experiments measured the CN group concentration, which provides direct information about the P2VP component. SIMS data, plotted in Figure 3a for the case PS host of $P = 15400$ ($P \gg N_{\text{PS}}$), reveal that the micelles are located preferentially at the free surface. For the sample containing PS host chains of $P = 125$, the micelles are more uniformly distributed throughout the sample, as expected due to the enhanced intermixing between the host chains and the corona of the micelles, as shown in Figure 3b. Note that the average sizes of the micellar cores estimated from SIMS profiles are consistent with those from STEM images.

In addition to the micelles, evidence of the brush layer is also clear from the SIMS profiles in both Figures. Since the depth resolution of SIMS is $\sim 15 \text{ nm}$, we prepared standards of known thicknesses and compared the normalized SIMS profiles of all the samples. This allowed us to accurately estimate the thickness of the brush layer. For the case of $P \gg N_{\text{PS}}$ (Figure 3a), the brush layer is approximately $h_{\text{brush}} = 19 \text{ nm}$. The brush layer of the other sample (Figure 3b) is necessarily smaller, as the host chains greatly penetrated into the brush. The dependence of h_{brush} is plotted as a function of P in Figure 4 (circles); h_{brush} increases with increasing P and appears to reach a plateau.

It turns out that another means by which the brush layer may be determined is to rinse the films with toluene (a poor solvent for P2VP), which removes the PS hosts, thereby exposing the

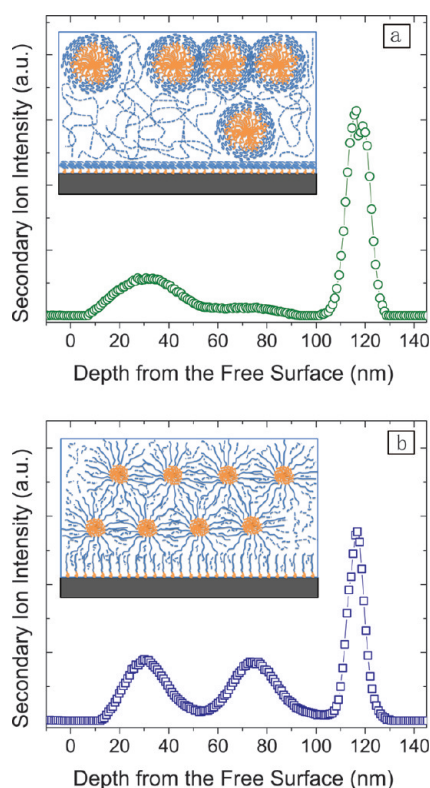


Figure 3. Depth profiles of P2VP in the PS-*b*-P2VP/PS ($P = 15\,400$) sample (part a), and of the PS-*b*-P2VP/PS ($P = 125$) sample (part b), measured by SIMS, are shown. The insets are schematics of the corresponding morphologies of the films.

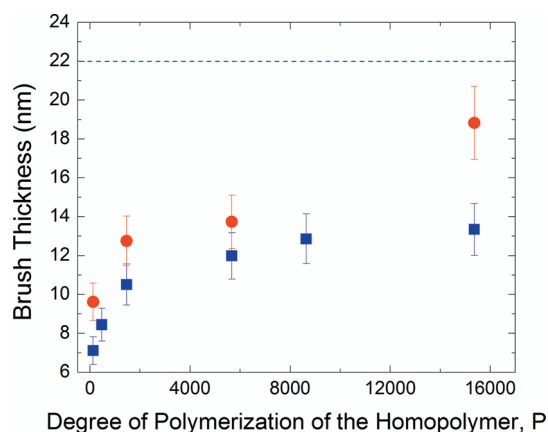


Figure 4. Brush layer thickness as a function of the molecular weight of host homopolymer. The circles represent the brush thicknesses measured using SIMS and the squares were determined from samples subjected to the toluene washing process. The dashed line represents the brush thickness of a pure PS-*b*-P2VP thin film supported on silicon nitride substrate.

underlying diblock brush layer. The thicknesses of the brush layers, h_{brush} , are plotted as a function of host PS molecular weight in Figure 4 (squares); h_{brush} increases with increasing P and approaches a plateau at high P . The maximum brush thickness P is consistent with the conclusions drawn from the SIMS data. Our experiments show that in the pure diblock copolymer the layer in contact with the substrate is of thickness $L/2 = L_{\text{PS}} + L_{\text{P2VP}} = 22\text{ nm} > h_{\text{brush}}$. Using the parameters mentioned earlier, we calculate the interlamellar

spacing, in the strong segregation limit, to be $L = aN^{2/3}\chi^{1/6} = 40\text{ nm}$, which agrees well with our experimental results. Recall that equilibrium of the system must be established between the copolymer chains in the micelles, those adsorbed onto the surface to form the brush layer and the free copolymer chains in the system. Hence the homopolymer chains would always exhibit some degree of intermixing with the PS components in the micelles and the brush layer. This implies that the brush in the blend is never pure even in the high P regime, so it never reaches the ideal (pure) copolymer case.

Comparisons between the structural organization of this system and that of polymer brush-grafted nanoparticles in a thin film homopolymer melt³¹ provide additional insight into the physics of tethered entities in confinement. In ref 31, we showed that for Au nanoparticles possessing a core diameter of 4.3 nm, onto which PS chains are grafted, in a PS melt, the transition between wet-brush to dry-brush occurred when $P/N = 1.5$; this transition is slightly higher than the predicted value of $P/N = 1$ for a planar surface. This is not unexpected; for a spherical surface the effective grafting density $\Sigma_{\text{sphere}} < \Sigma_{\text{planar}}$; hence the lower effective grafting density, associated with the curvature of the nanoparticles, is responsible for shifting the transition to a larger value of P/N . This would lead to enhanced miscibility. Since the curvature of the micelles is much smaller than that of the tethered nanoparticles, the shifting of the transition from $P/N > 3$, cannot be rationalized in terms of the shape of the micelles.

The images in Figures 1 and 2 indicate that the micellar core size is constant, and largest for $P > 3N_{\text{PS}}$, but it decreases with decreasing P . The decrease is, in part, consistent with enhanced intermixing between the host chains and the micelle coronas with decreasing P (recall that the penetration depth $\lambda \sim N/P$).³⁰ The chains that compose the corona would stretch in order to accommodate intermixing with the free P -mer host chains; concurrently the P2VP blocks in the core would have to become compressed in order to maintain a constant segmental density. There is however an important additional contribution to the decrease of the micelle core diameter, which we now discuss.

We begin by noting that a fundamental difference between the spherical micelle system and the chain end-tethered hard spheres: the grafting densities, Σ_0 , as well as the core size, of the chain end-tethered hard spheres are fixed, whereas the micelle core size decreases with decreasing P . We determined that in the regime $P_m > 3N_{\text{PS}}$, where the average micelle diameter remains constant, $D = 44\text{ nm}$, the micelle “grafting density” (the total number of PS blocks in one micelle/surface area of the core) is $\Sigma_{\text{micelle}} = 0.17\text{ chains/nm}^2$. The values of the “grafting densities” for mixtures containing the three lowest values of P are $\Sigma_{\text{micelle}} = 0.09, 0.11$, and 0.14 chains/nm^2 , for $P = 125, 470$, and 1460 , respectively. For these calculations, we used the experimentally determined D_{core} to calculate the volume of the core, from which the number of copolymer chains in a micelle was determined ($M_n(\text{P2VP}) = 29100\text{ g/mol}$; density of P2VP is 1.18 g/cm^3 , density of PS is 1.045 g/cm^3). This enabled the calculation of Σ_{micelle} . Clearly, the “grafting density” Σ_{micelle} of the micelles decreased as the size of the P -mer host chains decreased.

On the basis of the foregoing, there appears to be two contributions to the reduction of the core size of the micelle: (1) reduction in the number of chains/micelle leading to the increase in the number of micelles (Figure 2); (2) stretching of the corona, due to intermixing, and the associated shrinking of the blocks that comprise the core. Evidently, the translational entropy of the free P -mer chains is enhanced with an increase in the number of micelles, and smaller micelles. The increase in

translational entropy appears to be larger than the cost due to the increased the total core/corona interfacial area, associated with the increasing number of micelles.

It was just shown that decrease of D_{core} with decreasing P (accompanied by an increase of n_{micelle}) is consistent with the notion that the micellar system has an ability to reduce the number of chains/micelle, and decreasing micellar size, as P decreases. In the regime $P > 3N_{\text{PS}}, D_{\text{core}} = \text{constant}$ and $\Sigma_{\text{micelle}} = 0.17 \text{ chains/nm}^2$. The grafting density of the tethered surface where the wet-brush/dry-brush transition occurred for $P/N \sim 1$ was $\Sigma_0 \sim 1.5 \text{ chains/nm}^2$, in other words $\Sigma_0 \gg \Sigma_{\text{micelle}}$. That this wet-brush to dry-brush transition occurred for $P = P_m \gg N_{\text{PS}}$, instead of $P^* \sim N_{\text{PS}}$, is not surprising. The size of the P -mer chains must necessarily be large in comparison to N_{PS} in order to reach the dry-brush condition for these smaller values of Σ_{micelle} compared to Σ_0 .

The interactions between the micelles are now further discussed in light of the behavior of chain end-tethered nanoparticles. In a thin film polymer brush-coated nanoparticle/homopolymer system, assuming the size of the nanoparticle cores is sufficiently large, and the brush is relatively short compared to the homopolymer host chains, the nanoparticles form close-packed aggregates and they segregate toward both the free surface and the substrate of the film.³¹ The data in Figure 1d–f show aggregation of micelles into close packed structures, at large P . There is no correlation between the positions of the micelles shown in Figure 1a–c. Note that it is only when the density of micelles is low that it becomes clear that local aggregates of micelle reside throughout the films. Semenov et al.^{18,24} used analytical mean field theory to calculate the interaction strength between micelles and found that there exists a long-range attraction between micelles when the host homopolymer molecular weight exceeds a critical value, $P > P^*$:

$$P^* \approx 0.66(1-f)^{4/3}N(\chi N)^{-1/9}f^{-2/9}(1-f^{1/3})^{-2/3}(1.74-f^{1/3})^{2/9} \quad (3)$$

where $N = N_{\text{PS}} + N_{\text{P2VP}}, f = N_{\text{P2VP}}/N$. The maximum energy of attraction U_{attr} is proportional to the diameter of the entire micelle, $D = D_{\text{core}} + 2h_{\text{corona}}$, suggesting an increasing micelle–micelle attraction with increasing micelle size. For our systems this prediction indicates that $P^* = 492 \sim N_{\text{PS}}$, suggesting that host molecular weight larger than 51 000 g/mol, the micelles should attract each other. However, micelle interactions (attraction, hence aggregation) were observed only for values of $P_m > 3N_{\text{PS}}$ instead of the predicted value of $P^* \sim N_{\text{PS}}$. The theory is, nevertheless, qualitatively correct in predicting the attraction between the micelles, which should occur at sufficiently large P .

In light of this discussion of micelle–micelle interactions, it is worthwhile to note that Matsen and Gardiner³² showed that there should exist a finite interfacial tension between the corona (brush) layers and the host chains, which should increase with increasing P . This would be another source of the long-range attraction between the micelles, as it leads to a reduction of the brush/free chain interfacial area. The attraction between the micelles would lead to the formation of close packed structures.^{18,24} In prior studies, we have observed the interfacial segregation of grafted spherical particles, despite the fact that the grafted chains and the host chains are of identical chemical structure.^{33,34} The segregation occurs because the host chains gain configurational entropy and the tethered chains suffer a smaller loss in conformational entropy than the linear chains when they reside at the interfaces. These are also the reasons that the micelles migrate to the free surface, as shown by the SIMS profile when $P \gg N_{\text{PS}}$.

CONCLUSIONS

We showed that in thin film PS-*b*-P2VP/PS mixtures, the copolymer chains form micelles, possessing an inner core of the P2VP-component and corona of the PS-component, within the PS host. The copolymer chains, in addition to forming micelles, also adsorb onto the substrate, with the P2VP-component exhibiting strong attraction, forming a brush layer. At equilibrium the chemical potential of copolymer chains in the micelles, μ_{micelle} , and at the substrate, $\mu_{\text{substrate}}$, as well as that of the free chains, μ_{free} , must be equal; this determines the size of the micelles and the thickness of the brush layer. The micellar core diameter, D_{core} , increased with increasing degree of polymerization of the homopolymer, P , and became constant at large P , under the dry-brush conditions. The increase in D_{core} was accompanied by a decrease in the number density of micelles; the number density of micelles reached a constant value at large P . Additionally, the copolymer brush layer thickness increased with increasing P , reaching a plateau at large P . In the large P regime, the micelles aggregated to form close packed structures and resided preferentially at the free surface in an effort to minimize the free energy of the system. In contrast to brush coated nanoparticle systems, where the grafting density, Σ_0 , is fixed, the micellar system has the ability to reduce the micellar size, in part by reducing the number of chains/micelle, and increasing the number of micelles, each of which possesses a lower “grafting” density. This has the effect of maximizing the translational entropy of the free host chains, while minimizing the overall free energy of the mixture. Future research involves considering a range of block copolymer architectures and surfaces and different film thicknesses. The development of theory to gain a quantitative understanding of the relative contributions to the free energy is planned. These predictions can be tested experimentally.

ACKNOWLEDGMENT

This research was supported by the National Science Foundation (NSF), Division of Materials Research, Polymers Program (DMR-0906425). The SIMS measurements were performed by Dr. Tom Mates, University of California, Santa Barbara. X.C.C. thanks members of the group Jenny Kim, for useful discussions about the micelle formation, and Emmanouil Glynos, for discussions about brush layers in solvents.

REFERENCES

- (1) Bates, F. S.; Fredrickson, G. H. *Annu. Rev. Phys. Chem.* **1990**, *41*, 525–557.
- (2) Green, P. F.; Russell, T. P. *Macromolecules* **1991**, *24* (10), 2931–2935.
- (3) Green, P. F.; Russell, T. P. *Macromolecules* **1992**, *25* (2), 783–787.
- (4) Shull, K. R.; Kramer, E. J.; Hadzioannou, G.; Tang, W. *Macromolecules* **1990**, *23* (22), 4780–4787.
- (5) Retsos, H.; Terzis, A. F.; Anastasiadis, S. H.; Anastassopoulos, D. L.; Toprakcioglu, C.; Theodorou, D. N.; Smith, G. S.; Menelle, A.; Gill, R. E.; Hadzioannou, G.; Gallot, Y. *Macromolecules* **2002**, *35* (3), 1116–1132.
- (6) Costa, A. C.; Geoghegan, M.; Vlcek, P.; Composto, R. J. *Macromolecules* **2003**, *36* (26), 9897–9904.
- (7) Green, P. F. *J. Polym. Sci., Part B: Polym. Phys.* **2003**, *41* (19), 2219–2235.
- (8) Brown, H. R.; Deline, V. R.; Green, P. F. *Nature* **1989**, *341* (6239), 221–222.
- (9) Oslanec, R.; Costa, A. C.; Composto, R. J.; Vlcek, P. *Macromolecules* **2000**, *33* (15), 5505–5512.

- (10) Ruzette, A.-V.; Leibler, L. *Nat. Mater.* **2005**, *4* (1), 19–31.
- (11) Yokoyama, H.; Kramer, E. J. *Macromolecules* **2000**, *33* (5), 1871–1877.
- (12) Dai, K. H.; Kramer, E. J. *J. Polym. Sci., Part B: Polym. Phys.* **1994**, *32* (11), 1943–1950.
- (13) Meli, L.; Li, Y.; Lim, K. T.; Johnston, K. P.; Green, P. F. *Macromolecules* **2007**, *40* (18), 6713–6720.
- (14) Zhan, Y.; Mattice, W. L. *Macromolecules* **1994**, *27* (3), 677–682.
- (15) Gohy, J. F. Block copolymer micelles. In *Block Copolymers II*; Springer-Verlag: Berlin, 2005; Vol. 190, pp 65–136.
- (16) Leibler, L.; Orland, H.; Wheeler, J. C. *J. Chem. Phys.* **1983**, *79* (7), 3550–3557.
- (17) Whitmore, M. D.; Noolandi, J. *Macromolecules* **1985**, *18* (12), 2486–2497.
- (18) Semenov, A. N. *Macromolecules* **1992**, *25* (19), 4967–4977.
- (19) Pepin, M. P.; Whitmore, M. D. *Macromolecules* **2000**, *33* (23), 8644–8653.
- (20) Uneyama, T.; Doi, M. *Macromolecules* **2005**, *38* (13), 5817–5825.
- (21) Cavallo, A.; Müller, M.; Binder, K. *Macromolecules* **2008**, *41* (13), 4937–4944.
- (22) Winey, K. I.; Thomas, E. L.; Fetters, L. J. *Macromolecules* **1991**, *24* (23), 6182–6188.
- (23) Shull, K. R.; Winey, K. I.; Thomas, E. L.; Kramer, E. J. *Macromolecules* **1991**, *24* (10), 2748–2751.
- (24) Esselink, F. J.; Semenov, A. N.; Tenbrinke, G.; Hadzioannou, G.; Oostergetel, G. T. *Phys. Rev. B* **1993**, *48* (18), 13451–13458.
- (25) Koizumi, S.; Hasegawa, H.; Hashimoto, T. *Macromolecules* **1994**, *27* (22), 6532–6540.
- (26) Floudas, G.; Hadjichristidis, N.; Stamm, M.; Likhtman, A. E.; Semenov, A. N. *J. Chem. Phys.* **1997**, *106* (8), 3318–3328.
- (27) Adediji, A.; Lyu, S.; Macosko, C. W. *Macromolecules* **2001**, *34* (25), 8663–8668.
- (28) Shull, K. R. *Macromolecules* **1993**, *26* (9), 2346–2360.
- (29) Oh, H.; Green, P. F. *Macromolecules* **2008**, *41* (7), 2561–2566.
- (30) Borukhov, I.; Leibler, L. *Macromolecules* **2002**, *35* (13), 5171–5182.
- (31) Chen, X. C.; Green, P. F. *Soft Matter* **2011**, *7*, 1192–1198.
- (32) Matsen, M. W.; Gardiner, J. M. *J. Chem. Phys.* **2001**, *115* (6), 2794–2804.
- (33) Meli, L.; Arceo, A.; Green, P. F. *Soft Matter* **2009**, *5* (3), 533–537.
- (34) Kim, J.; Green, P. F. *Macromolecules* **2010**, *43* (3), 1524–1529.